The Plant Cell, Vol. 11, 1239–1252, July 1999, www.plantcell.org © 1999 American Society of Plant Physiologists

Gnarley1 Is a Dominant Mutation in the *knox4* Homeobox Gene Affecting Cell Shape and Identity

Toshi Foster,[a] Judy Yamaguchi,[a] Bryan C. Wong,[a] Bruce Veit,[b] and Sarah Hake[a,c,1]

[a] Department of Plant and Microbial Biology, University of California, Berkeley, California 94720
[b] Institute of Molecular Biosciences, Massey University, Palmerston North, New Zealand
[c] Plant Gene Expression Center, U.S. Department of Agriculture, Agricultural Research Service, Albany, California 94710

Maize leaves have a stereotypical pattern of cell types organized into discrete domains. These domains are altered by mutations in *knotted1* (*kn1*) and *knox* (for *kn1*-like homeobox) genes. *Gnarley* (*Gn1*) is a dominant maize mutant that exhibits many of the phenotypic characteristics of the *kn1* family of mutants. *Gn1* is unique because it changes parameters of cell growth in the basal-most region of the leaf, the sheath, resulting in dramatically altered sheath morphology. The strongly expressive allele *Gn1-R* also gives rise to a floral phenotype in which ectopic carpels form. Introgression studies showed that the severity of the *Gn1*-conferred phenotype is strongly influenced by genetic background. *Gn1* maps to *knox4*, and *knox4* is ectopically expressed in plants with the *Gn1*-conferred phenotype. Immunolocalization experiments showed that the KNOX protein accumulates at the base of *Gn1* leaves in a pattern that is spatially and temporally correlated with appearance of the mutant phenotype. We further demonstrate that *Gn1* is *knox4* by correlating loss of the mutant phenotype with insertion of a *Mutator* transposon into *knox4*.

INTRODUCTION

Leaves are useful in the study of plant morphogenesis because their development is easily described in terms of well-defined growth axes. The growth associated with these axes as well as the temporal sequence in which the tissue and cellular identities of the leaf become defined are conveniently described in terms of the plastochron, which is the interval of time between successive leaf initiation events. Morphological analysis suggests that asymmetry in the transverse dimension (abaxial to adaxial) is determined by plastochron 1 (P_1), that is, as soon as a leaf primordium emerges from the flank of the shoot apical meristem (Kaplan, 1973). In most dicots, differentiation of the midrib and margin defines central and lateral domains in the leaf primordia by P_3 (McHale, 1993). Leaflets, lobes, stipules, tendrils, and other features that distinguish regional identity along the proximal–distal axis become apparent between P_2 and P_5 (Kaplan, 1973; Marx, 1987; Steeves and Sussex, 1989).

The vegetative leaf of maize has been described extensively and is well suited for the study of plant development (Sharman, 1942; Poethig, 1984; Sylvester et al., 1990). Four distinct domains differentiate along the proximal–distal axis of the leaf: distal blade, proximal sheath, and between them, auricle and ligule. These domains are apparent by P_4 to P_6, although they are probably initiated earlier (Sylvester et al., 1990). Each of these subdomains of the leaf has a unique morphology and anatomy that are adapted for a particular function.

The distally positioned blade extends away from the shoot and functions as the major photosynthetic organ of the plant. Approximately five to 20 lateral veins are present on either side of the central midrib, and 12 to 30 intermediate veins are found between each lateral vein (Russell and Evert, 1985). Vascular elements in the blade are located midway between adaxial and abaxial epidermal surfaces and exhibit Krantz anatomy, which facilitates photosynthesis in hot, dry climates (Brown, 1975). By contrast, the proximally positioned sheath is a thick tissue that wraps around the culm of the plant to provide mechanical support. Vascular bundles in the sheath do not exhibit Krantz anatomy, and they are appressed against the abaxial epidermis (Russell and Evert, 1985).

The wedge-shaped auricle forms a hinge between blade and sheath. Leaves that lack an auricle, such as the recessive *liguleless* mutations (Becraft et al., 1990; Harper and Freeling, 1996), are more upright than normal leaves. Auricle tissue is thicker than blade tissue but thinner than sheath tissue in the transverse dimension. Intermediate veins fuse with lateral veins at the border between blade and auricle such that only one or two intermediate veins are found between adjacent lateral veins in both the auricle and sheath (Sinha and Hake, 1994). The ligule is an epidermally derived

[1] To whom correspondence should be addressed. E-mail maizesh@nature.berkeley.edu; fax 510-559-5678.

fringe of tissue located between the auricle and sheath on the adaxial side of the leaf (Sharman, 1942).

Analyses of mutants that are altered in leaf shape demonstrate some of the mechanisms that regulate normal leaf development (reviewed in Sylvester et al., 1996; Nelson and Dengler, 1997; Poethig, 1997). Analysis of the *narrow sheath* mutant suggests the presence of discrete central and lateral domains of the maize leaf that are established early in leaf development (Scanlon et al., 1996). Other mutants have been described, and these appear to interfere with patterning of the leaf along the proximal–distal axis. For example, the dominant morphological mutants *Knotted1* (*Kn1*), *Rough Sheath1* (*Rs1*), *Liguleless3* (*Lg3*), and *Lg4* all show patches of ligule and sheath-like tissue in more distal regions of the leaf (Freeling and Hake, 1985; Becraft and Freeling, 1994; Sinha and Hake, 1994; Fowler and Freeling, 1996). *Kn1*, *Rs1*, and *Lg3* are caused by mutations to related homeobox genes, termed *knox* (for *kn1*-like homeobox; Hake et al., 1989; Schneeberger et al., 1995; Fowler and Freeling, 1996). The expression of *kn1* and other *knox* genes in the meristem suggests that plant homeobox genes function in shoot meristems (Smith et al., 1992; Jackson et al., 1994). Loss-of-function phenotypes for *kn1* (Kerstetter et al., 1997) and a related Arabidopsis gene, *SHOOT MERISTEMLESS* (Long et al., 1996), support this role for *knox* genes.

In this study, we introduce a new dominant morphological mutant, *Gnarley1* (*Gn1*), that, like other members of the *kn1* family, displays alterations in the ligule region. *Gn1* is unique due to cell shape changes in the sheath and internode and the presence of a floral phenotype. *Gn1* maps to *knox4*, and *Gn1-R* (*R* for reference allele) mutants ectopically express the KNOX protein in a pattern consistent with morphological alterations to the sheath. The *knox4* transcript is expressed in *Gn1-R* leaves but not in normal leaves. In a screen for loss of the dominant phenotype in a *Mutator (Mu)* background, we obtained an insertion into *knox4*, thereby proving that *Gn1* is *knox4*.

RESULTS

Gn1 Is a Spontaneous, Dominant Mutant Defined by Two Alleles

Gn1-R is a spontaneous mutation that was recovered by T. Pryor (Commonwealth Scientific Industrial Research Organization, Canberra, Australia) in 1990 and subsequently was mapped to chromosome 2L (Foster and Hake, 1994) by using *waxy* translocations (Laughnan and Gabay-Laughnan, 1993). A mutation with a similar phenotype, *Lg–9167*, also mapped to this region (G. Muelbauer and M. Freeling, personal communication). To determine whether *Gn1-R* and *Lg–9167* might be allelic, we crossed the double heterozygote to normal (*gn1*+) plants, and the phenotype of the progeny was scored. All 264 scored progeny were mutant, indicating that *Gn1-R* and *Lg–9167* map to within 0.4 map units of one another and are likely to be alleles. *Lg–9167* was renamed *Gn1-S* for D. Schwartz (University of Indiana, Bloomington, IN), who provided the seed stock.

Cell Shape Changes Correlate with Altered Leaf Morphology in *Gn1-R* Mutants

To elucidate the primary defect of the *Gn1* mutation and determine phenotypic variability due to genetic background, we introgressed *Gn1-R* and *Gn1-S* mutants into inbred lines B73, A188, and W22 for four to six generations. The most obvious aspect of the *Gn1-R*–conferred phenotype is reduced plant height compared with normal siblings, as shown in Figure 1A. With the exception of the first few internodes, the proportional reduction in *Gn1-R* internodal length is roughly constant for each internode in both B73 and W22, as shown in Figures 2A and 2B. Thus, the reduction in *Gn1-R* plant height is due to a reduction of each internode rather than to a reduction of specific internodes or deletion of internodes. Overall, *Gn1-R* plants introgressed into W22 had 36% of sibling height, whereas B73 *Gn1-R* plants had 83% of sibling height, indicating that genetic background affects the plant stature of *Gn1-R* mutants (Figure 3A). *Gn1-S* plants were not significantly shorter than normal siblings (data not shown). Compounding the reduced internode length of *Gn1-R* plants is the curving nature of the culm, giving the plants a twisted appearance (Figure 1B).

The leaf shape of *Gn1* mutants was assessed in introgressed families of *Gn1-R* and *Gn1-S* mutants by measuring the length (tip to base) and width (margin to margin) of sheath and blade (Table 1). A comparison of *Gn1-R*, *Gn1-S*, and normal sheath measurements indicated that *Gn1-R* sheaths are significantly shorter and wider than normal sheaths. In W22, for example, *Gn1-R* sheaths are $<$50% of the length and 150% of the width of nonmutant sheaths (Figure 3B). In the same genetic background, *Gn1-S* sheaths are 90% of the length and 113% of the width of normal leaves. The width and length of the leaf blades were less affected, with little or no difference measured for *Gn1-R* and *Gn1-S*, respectively (Table 1).

To investigate the cause of the abnormally short internodes and sheaths of *Gn1-R* mutants, we measured cell sizes from replicas made of the surfaces of internode 10 and the corresponding sheath. In a W22 background, mutant epidermal cells from internode and sheath were approximately half the length of those in normal siblings, whereas in a B73 background, they were approximately three-fourths the normal length (Figure 3C). The reduction in cell length is comparable in magnitude to the reduction in overall plant height—36 and 83% for W22 and B73, respectively. These data suggest that the reduction in internode and sheath length observed in *Gn1-R* mutants is caused by an overall reduction in cell length in those tissues.

Figure 1. The *Gn1-R* Mutation Has Pleiotropic Effects on Culm Development.

(A) *Gn1-R* mutants (left) are reduced in stature compared with nonmutant siblings (right).
(B) *Gn1-R* culms often twist and bend, causing the phyllotaxy to appear abnormal.
(C) Abaxial view of a *Gn1-R* sheath exhibiting extreme distortion of sheath tissue. This tissue buckling is caused by localized regions of sheath thickening interspersed with thinner tissue.
(D) *Gn1-R* (left) and normal sibling (right) female inflorescences surrounded by sheathlike husk leaves. Note how the tip of the *Gn1-R* ear protrudes from the husk leaves, whereas the husk leaves completely cover the tip of the normal ear.

Examination of cross-sections through *Gn1-R* sheath tissue reveals defects in histological organization. Vascular bundles are normally appressed against the abaxial epidermis and are associated with an abundance of very lignified tissue, called sclerenchyma (Figure 4D). In *Gn1* sheaths, the vascular bundles are placed in a more median position in the tissue, and the hypodermal sclerenchyma is not continuous with the abaxial epidermis. *Gn1* sheath tissue is also abnormally thick in the transverse (adaxial–abaxial) dimension (Figure 4C). Proliferation and expansion of mesophyll cells primarily in the abaxial layer of *Gn1* sheaths appear to cause the abnormally thickened sheath tissue. The expansion is variable in expression; localized regions of expanded cells interspersed with more normal tissue give the *Gn1* sheaths a rumpled or corrugated appearance (Figure 1C). The replica images also reveal patches of sheath epidermal cells with abnormal shapes (contrast Figures 4A and 4B). These irregularly shaped epidermal cells are concentrated in regions of convoluted tissue and occur sporadically in patches across the sheath.

Husk leaves, which enclose the female inflorescence, are mostly sheath, depending on genetic background. The husks of *Gn1-R* plants are very short and display severe convolutions. Because the husks are so short, the ears often protrude from the husks (Figure 1D).

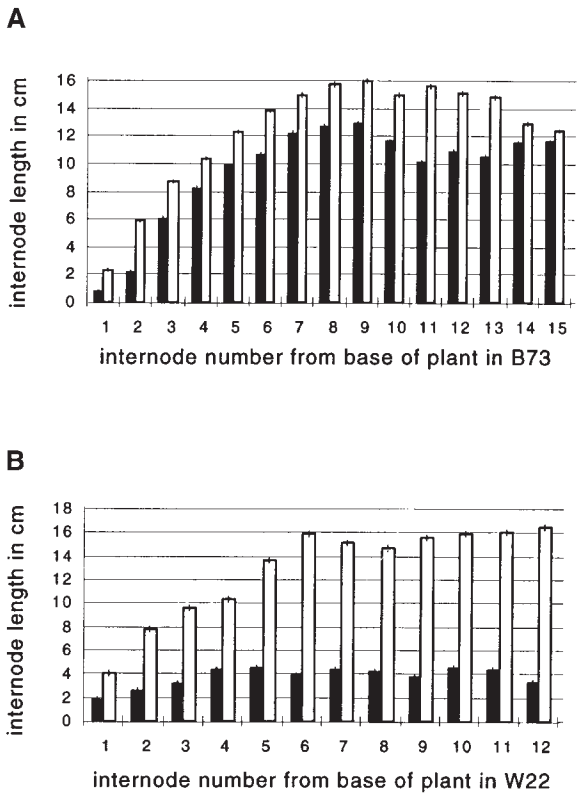

Figure 2. The Reduced Height of *Gn1-R* Mutants Is Caused by an Overall Reduction in Internode Lengths.

Each bar represents the average internode length for 10 comparable internodes of *Gn1-R* (black bars) or normal siblings (white bars). Vertical lines represent the standard error of the averaged number. With the exception of the first few internodes, the overall reduction in *Gn1-R* is consistent within a given introgressed line.
(A) B73 background.
(B) W22 background.

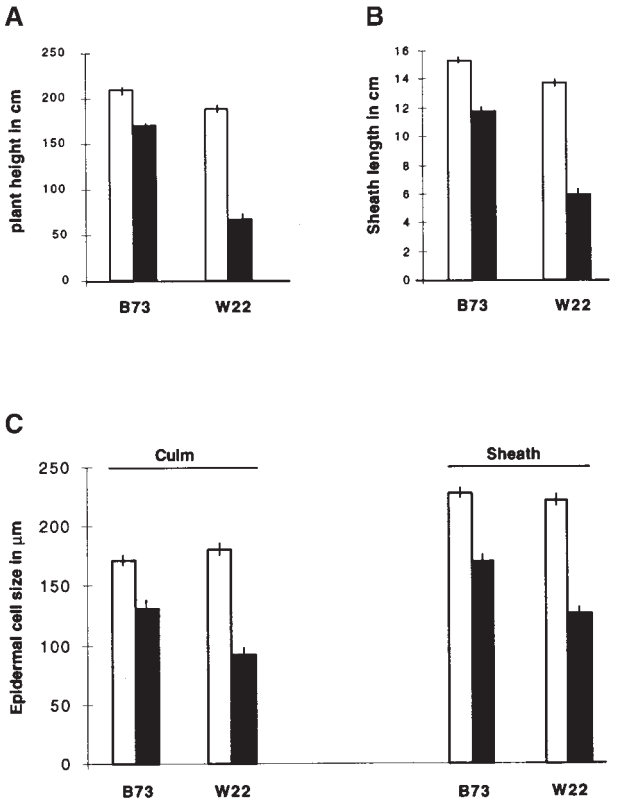

Figure 3. Plant Height Is Correlated with Cell Length.

(A) Each bar represents the average plant height for 20 *Gn1-R* or normal siblings within a given introgressed line. Vertical lines represent the standard error of the averaged number.

(B) Each column represents the average sheath length of leaf 10 for 20 individuals, as described in Table 1. As shown for overall plant height, *Gn1-R* mutants introgressed into W22 are the most reduced in sheath length. Vertical lines represent the standard error of the averaged number.

(C) Epidermal replicas were made of the internode and sheath of leaf 10 for *Gn1-R* and nonmutant siblings within a given genetic background. Epidermal peels from the adaxial epidermis of *Gn1-R* and nonmutant sheath tissue were compared. At least 80 cells from each epidermal replica were measured along their long axis by using National Institutes of Health Image software. Each column represents an average cell length, and the vertical lines represent the standard error of the averaged number. The reduction in cell length of sheath and internode appears proportionally similar to the reduction in overall sheath and internode lengths within a given inbred background.

The data for *Gn1-R* are shown as black bars and the data for normal siblings as white bars.

Irregular Blade–Sheath Boundary in *Gn1* Mutants

The ligule forms at the boundary between sheath and blade (Figure 5A). Using a replica technique for scanning electron microscopy (SEM), Sylvester et al. (1990) have shown that the ligule is initiated on the adaxial epidermis from two foci on either side of the midrib. These foci spread in a horizontal line toward both margins (Figure 5C). In *Gn1-R* mutants, the ligule does not form in a straight horizontal line; instead, it is always positioned more distally in tissue flanking the midrib than over the midrib itself and frequently extends toward the margins in a jagged line (Figure 5B). Scanning electron microscopic analysis of the adaxial surface of P_5 leaves indicates that the *Gn1-R* ligule is irregular at the first visible sign of ligule outgrowth (Figure 5D). These data indicate that the irregular position of the *Gn1-R* ligule represents an early defect in the patterning of the leaf rather than the result of differential growth across the lateral dimension of the leaf.

We examined the histology of *Gn1-R* blades in regions with altered ligule position. In normal leaves, auricle cells are found immediately distal to the ligule, between the ligule and blade (Figure 5E). In regions of *Gn1-R* leaves in which the ligule position is altered, auricle cells are absent and sheath cells spread distally into blade regions, as determined by scanning electron microscopic analysis of adaxial leaf surfaces (Figure 5G). A horizontal cross-section through such a region illustrates that the internal anatomy is also very sheathlike. Large mesophyll cells make the tissue thicker in the transverse dimension than in the adjacent blade tissue (Figure 5F). Within this thickened region, the vascular bundles are appressed against the abaxial surface and are associated with abaxial hypodermal sclerenchyma, similar to normal sheath. These observations indicate that regions within *Gn1-R* blades have histological characteristics of normal sheath tissue and that the ligule signifies a consistent boundary between sheath and blade despite its erratic positioning.

The auricle extends from both sides of the midrib to the leaf margins in wild-type leaves (Figure 6A, center). Intermediate and smaller veins anastomose into lateral veins at the ligule–auricle boundary such that only one or two intermediate veins exist between lateral veins in the sheath (Sharman, 1942) (Figure 6B). In *Gn1-R* and *Gn1-S* mutants, the auricle does not extend to the midrib but stops some distance from the midrib (Figure 6A, arrow at left). In mutants with a severe *Gn1*-conferred phenotype, the auricles are reduced to the very leaf margins or are eliminated altogether (Figure 6A, right). In *Gn1-R* mutants, many of the smaller veins do not anastomose at the ligular region, leading to an abundance of smaller veins that persist into the sheath. Many of these smaller veins eventually anastomose, but they do so over a much longer region than normal (Figure 6C, arrows).

Extra Carpels Form in *Gn1-R* Pistillate Flowers

Maize is a monoecious plant with a single, terminal, staminate (male) inflorescence and several pistillate (female) inflorescences in lateral positions. Male and female floral development is similar until differential abortion of male or female organs results in unisexual flowers (Cheng et al., 1983; Veit et al., 1993). The maize pistil contains a unilocular

Table 1. Averaged *Gn1* Leaf Dimensions as a Fraction of Normal Siblings[a]

		Blade[b]		Sheath[b]	
Background	Allele	Length	Width	Length	Width
B73	*Gn1-R*	1.00 ± 0.01	1.09 ± 0.01	0.77 ± 0.01	1.11 ± 0.01
	Gn1-S	0.98 ± 0.01	1.12 ± 0.01	0.96 ± 0.01	0.99 ± 0.01
A188	*Gn1-R*	0.87 ± 0.01	1.21 ± 0.01	0.74 ± 0.01	1.32 ± 0.01
	Gn1-S	0.98 ± 0.02	1.03 ± 0.01	0.98 ± 0.01	1.06 ± 0.01
W22	*Gn1-R*	0.77 ± 0.01	1.27 ± 0.01	0.43 ± 0.01	1.47 ± 0.01
	Gn1-S	0.95 ± 0.02	1.15 ± 0.01	0.90 ± 0.02	1.13 ± 0.01

[a] Leaf 10 was measured for 20 mutant and normal siblings within each introgressed line.

[b] Blade length was measured along the leaf margins from the ligule to the blade tip. Sheath length was measured along the margins from the node to the ligule. Both blade and sheath width were measured at their midpoints. Measurements were averaged, and average *Gn1* dimensions are represented as a fraction of average normal value. Standard error was calculated using a Taylor first-order expansion for estimating errors of nonlinear estimates.

ovary surrounded by three carpels. Two of the carpels fuse and elongate to form the stigma and style, which is known as the silk (Randolph, 1936; Irish and Nelson, 1993). The point of fusion is known as the stylar canal (Figure 7A). The three stamen primordia surrounding the pistil arrest early in their development as the silk initiates growth.

In female flowers of *Gn1-R* mutants, extra carpelloid organs develop from the base of the pistil (Figure 7B). These structures are developmentally retarded compared with the normal pistil, and they first appear after the outgrowth of the silk from the central pistil (data not shown). Eventually, these structures form a stylar canal and bivalvate silk, and they have an overall morphology similar to that of a normal pistil (Figure 7B). We quantified the frequency and total number of the carpelloid organs in three different genetic backgrounds. Thirty-seven and 83% of the florets had extra carpelloid structures in an A188 and W22 background, respectively. *Gn1-R* mutants introgressed into B73 did not make any carpelloid organs, although 10% had a rudimentary carpel, which was not suppressed, resulting in a univalvate silk in addition to the normal silk (data not shown).

To determine the extent of similarity between the carpelloid organs of *Gn1-R* and normal pistils, we used a carpel-specific gene, *zag2* (for *Zea mays AGAMOUS*), for in situ hybridization experiments (Schmidt et al., 1993). *zag2* is expressed in the supernumerary structures in a pattern identical to that of a normal pistil (Figures 7C and 7D). These structures develop an internal cavity surrounded by tissue that resembles the ovary wall. Although these structures have many attributes of normal pistils, they are not fertile, and there is no evidence that they contain an ovule (data not shown). The remnants of the carpelloid organs can often be found at the base of mature seeds from *Gn1-R* ears (data not shown). *Gn1-S* mutants do not have any obvious floral phenotype.

We crossed *Gn1-R* to two different floral mutants to further pursue identity of the carpelloid structures. The *silkless* (*sk*) mutation inhibits the elaboration of silks, rendering homozygous *sk*/*sk* individuals female sterile (Jones, 1925; Veit et al., 1993). Double mutants of *Gn1-R* and *sk* lack silks; however, they still exhibit the carpelloid structures, suggesting that these supernumerary structures are pistils. The stamens of pistillate flowers carrying the *silky* (*si*) mutation are not arrested as they are in normal development; instead, they are converted into sterile pistils (Fraser, 1933). *Gn1-R*/+ *si*/*si* double mutants have an average of 5.1 pistillate organs per floret, whereas *si*/*si* mutants have only three extra pistillate organs per floret and *Gn1-R* mutants have an average of 2.4. This additive interaction suggests that *Gn1-R* and *si* act independently and that the carpelloid structures in *Gn1-R* florets are not transformed stamens.

Ectopic Expression of the KNOX Protein in *Gn1-R* Leaves

Low-stringency hybridization with the homeobox portion of the *kn1* cDNA revealed 10 to 15 other *knox* genes in maize. These genes subsequently were isolated and mapped using recombinant inbred lines (Vollbrecht et al., 1991; Kerstetter et al., 1994). P-11, a genomic clone corresponding to *knox4*, mapped to position 162 on chromosome 2L (Kerstetter et al., 1994). Cosegregation data revealed that *knox4* and *Gn1-R* are tightly linked (Foster and Hake, 1994; data not shown).

Class 1 *knox* genes, such as *knox4*, *knox3*, *kn1*, and *rs1*, are expressed in meristems but not in leaves (Jackson et al., 1994; Kerstetter et al., 1994). Ectopic expression in leaves has been shown to be responsible for the dominant mutations *Kn1* and *Rs1* (Smith et al., 1992; Schneeberger et al., 1995). To determine whether ectopic KNOX expression occurred in *Gn1-R* plants, we incubated tissue sections of *Gn1-R* and wild-type seedlings with a polyclonal antiserum that recognizes KNOX proteins (Scanlon et al., 1996). Figure 8A shows KNOX protein localization to shoot apical meristem

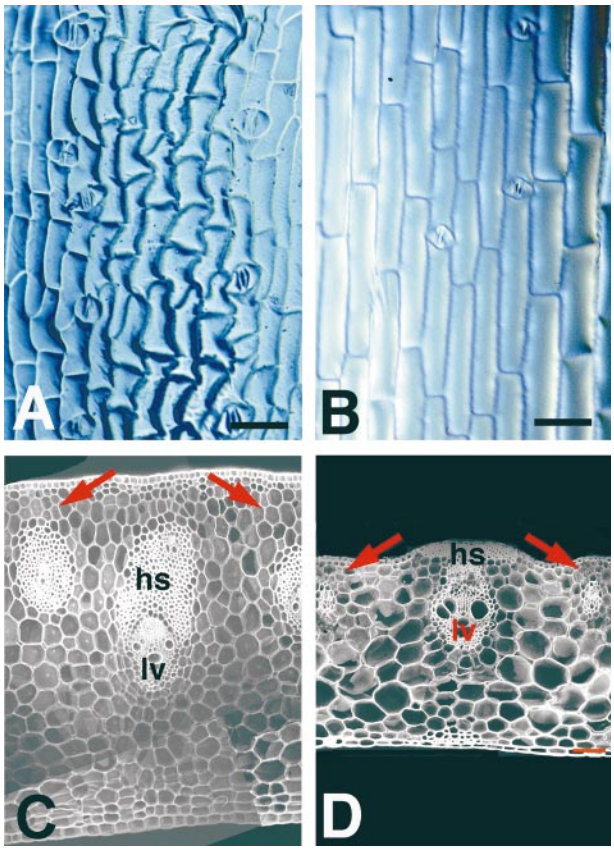

Figure 4. *Gn1* Mutant Sheath Tissue Exhibits Abnormal Histology.

(A) Epidermal replica of the adaxial surface of *Gn1-R* sheath. *Gn1-R* sheath cells are shorter and more irregularly shaped than are wild-type sheath cells.

(B) Epidermal replica of the adaxial surface of wild-type sheath.

(C) Confocal image of a cross-section through *Gn1-R* sheath tissue, with the abaxial surfaces oriented toward the top. The vascular bundles are not appressed against the abaxial surface, and the hypodermal sclerenchyma associated with each vascular bundle is not continuous with the abaxial surface.

(D) Confocal image of a cross-section through sheath tissue of a normal sibling. The vascular bundles are appressed against the abaxial surface and are associated with hypodermal sclerenchyma that is continuous with the epidermis.

hs, hypodermal sclerenchyma; lv, lateral vein. Bars in **(A)** and **(B)** = 80 μm.

nuclei but not leaf nuclei in wild-type seedlings. In similar transverse sections of *Gn1-R* seedlings, the anti-KNOX antibody detected the KNOX protein in nuclei of mutant leaves as well as the shoot meristem (Figure 8B). Expression of KNOX proteins in the *Gn1-R* meristem was excluded from cells in P_0, the region of the meristem predicted to form the next leaf, but was detected in leaves as early as P_1 (Figures 8D to 8F). The KNOX protein(s) accumulates at the base of *Gn1-R* leaves (Figures 8E and 8F), with the signal being most intense near the midrib and toward the abaxial side of the leaf (Figures 8B and 8D). The anti-KNOX antibody detected ectopic KNOX expression in both epidermal and mesophyll cells but not in vascular elements (Figure 8C). This expression persisted until P_6 to P_8 (data not shown). The pattern of ectopic KNOX expression in *Gn1-R* leaves coincides with the focus of the mutant phenotype near the midrib and at the base of the leaf.

To determine whether the ectopic KNOX expression was specifically *knox4*, we isolated a cDNA corresponding to *knox4* (CP11-5). Sequence comparison with other *knox* genes showed that KNOX4 was very similar to RS1 (Figure 9). Gene-specific probes were prepared from the 3′ ends of both *knox4* and *rs1*, and the extent of their cross-hybridization was determined (see Methods). RNA gel blot analysis was performed using 20 μg of total RNA isolated from young leaves and 10 μg of total RNA isolated from meristem-enriched tissue from *Gn1-R* seedlings and normal-appearing siblings. The meristem-enriched sample included young leaf primordia and leaf bases. Figure 10 shows that the transcript hybridizing with the *knox4* 3′ probe accumulates in *Gn1-R* leaves (lanes 4). The intensity of hybridization in the mutant leaves is approximately equal to the hybridization intensity detected in the meristem-enriched tissue. Reprobing the blot with a *rs1* 3′ probe, we detected some transcript in *Gn1-R* leaves; however, the intensity of hybridization was much less than that detected in the meristem RNA samples by the *rs1* probe. Based on the cross-hybridization of the *rs1* probe with the *knox4* cDNA (data not shown), we believe the *rs1* expression in *Gn1-R* leaves is due to cross-hybridization; however, we cannot rule out the possibility that some *rs1* is expressed in *Gn1-R* leaves.

Mu Insertions in *knox4* Revert the Dominant Phenotype

Gn1-R and *Gn1-S* have unique polymorphisms 5′ of the coding region that distinguish them from from their respective progenitors (data not shown). To further prove that *Gn1* is indeed due to a mutation in *knox4*, we crossed *Gn1-R* into a line carrying active *Mu* elements (Robertson, 1978; Chandler and Hardeman, 1992). Individuals that were homozygous for *Gn1-R* were identified based on *knox4* polymorphisms and used in outcrosses to wild-type females. The resulting 30,000 progeny were screened for loss of the *Gn1-R*–conferred phenotype. Of the 17 normal-appearing individuals that were obtained, three had the same polymorphisms of *Gn1-R* at the linked restriction fragment length polymorphism, *bnl17.14*, and were considered possible revertants.

DNA gel blot analysis was used to determine whether alterations had occurred in *knox4* coincident with loss of the *Gn1-R*–conferred phenotype. Figure 11 shows that *Gn1-R*–specific polymorphisms were altered in the 5′ end of the gene for one of the revertants but not the 3′ end of the gene. For example, when the 5′ probe and SstI-digested DNA were used,

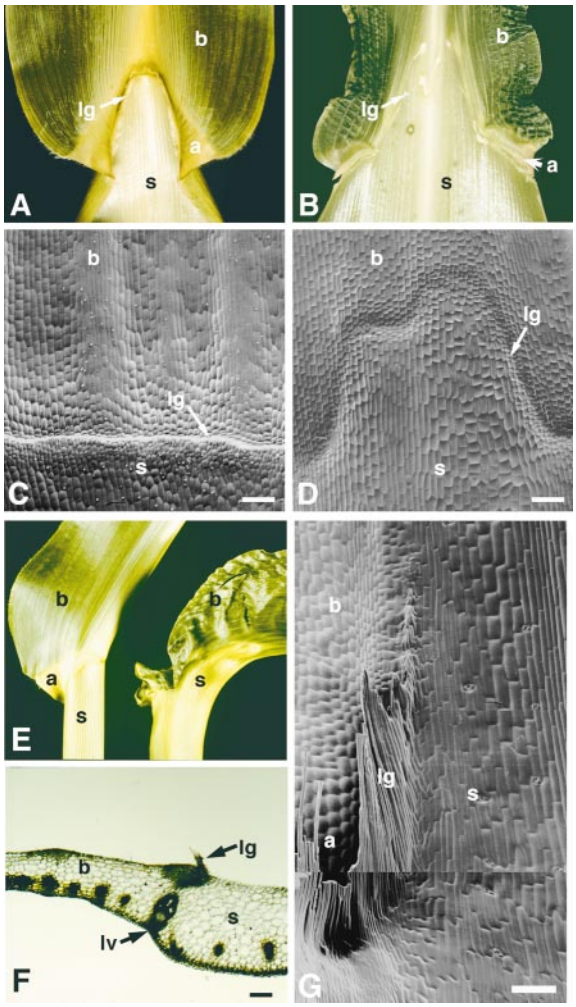

Figure 5. Comparison of the Ligular Regions of a Wild-Type and a *Gn1-R* Maize Leaf.

(A) Adaxial view of a wild-type leaf. The ligule extends horizontally across the leaf in a straight line and subtends the auricle, which is a wedge-shaped tissue that extends from either side of the midrib toward both margins.

(B) Adaxial view of a *Gn1-R* leaf. The *Gn1-R* ligule is irregularly shaped, and the auricle is reduced in the lateral dimension.

(C) and **(D)** SEM of the developing ligular region on the adaxial epidermis of a wild-type leaf during P_7 **(C)** and a *Gn1-R* leaf **(D)**. The irregular position of the *Gn1-R* ligule represents an early defect in the patterning of the leaf rather than the result of differential growth across the lateral dimension of the leaf.

(E) Abaxial view of the ligular regions of a wild-type (left) and a *Gn1-R* (right) leaf, illustrating that the auricle is missing and that regions of basal *Gn1-R* blade are transformed into sheath.

(F) A transverse hand-section of a *Gn1-R* leaf shows an abrupt transition from blade to sheathlike tissue that is bordered by a fringe of ligule. The sheathlike tissue is thicker than the blade, with the veins located toward the abaxial surface.

(G) SEM analysis of adaxial epidermis of a *Gn1-R* leaf reveals that cells in the transformed region have sheath characteristics, whereas cells in the untransformed region have blade characteristics.

In both **(F)** and **(G)**, the ligule forms at the boundary between transformed and untransformed tissue. This boundary is often coincident with a lateral vein. a, auricle; b, blade; lg, ligule; lv, lateral vein; s, sheath. Bars in **(C)** and **(D)** = 100 μm; bars in **(F)** and **(G)** = 250 μm.

the *Gn1-R*–specific band of ~3 kb was changed to a 4.8-kb band in the revertant, and the 8.45-kb EcoRV band that is present in *Gn1-R* was changed to 6 kb in the revertant. These results suggest that an insertion of ~1.8 kb increased the size of the SstI fragment and that the insertion contains an EcoRV site. Polymerase chain reaction (PCR) was used to determine the specific location of the insertion. Primers specific to *knox4* and the ends of *Mu* amplified a product that was cloned and sequenced. Sequencing revealed the insertion of a *Mu* element 21 bp 5′ of the start of *knox4* transcription. Further proof was obtained by showing that the *knox4* expression in *Gn1-R* leaves was missing in leaves from individuals homozygous for the *Mu* insertion (Figure 10, lanes 3). Thus, screening for a loss of the dominant *Gn1*-conferred phenotype led to the isolation of a *Mu* element insertion in *knox4* and proof that *knox4* is *Gn1*.

DISCUSSION

To gain insight into how large-scale pattern domains within the leaf become determined, we have undertaken a detailed morphological analysis of *Gn1*, a mutant in which both the shape and organization of these domains are disturbed. Our analysis indicates that these changes reflect altered development at both the cellular and supracellular levels. These alterations are correlated with ectopic expression of the KNOX class of proteins. It appears that the sheath responds to ectopic KNOX expression by alterations in cell shape, whereas the sheath–blade boundary responds by a cell fate change. We have also shown that *Gn1* is *knox4*, thus providing a tool to study the effects of *Gn1* on leaf development.

Cell Shape Changes and Their Influence on Leaf Shape

The sheath portion of *Gn1* leaves is shorter and wider than the sheath in normal leaves. Husk leaves, which are considered homologous to the sheath portion of the vegetative leaf, are similarly affected by *Gn1*. The basal regions of other leaflike organs, such as glumes, lemma, and palea, are completely unaffected. From measurements of epidermal cell length, it appears that the internode and sheath cells are shorter to the same degree that the internode and sheath are shortened.

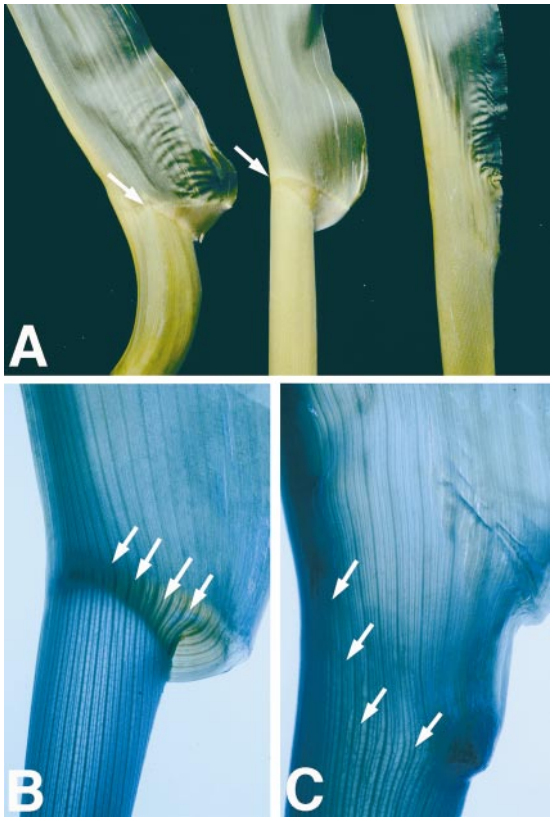

Figure 6. The *Gn1* Mutation Interferes with Auricle Development.

(A) Abaxial views of the auricle region of a wild-type leaf (center) and two *Gn1-R* mutants, showing the range of phenotypic severity. Note that the auricle extends to the midrib in the wild-type leaf but stops some distance from the midrib in the *Gn1-R* mutant at left (cf. arrows). The auricle is eliminated altogether from the *Gn1* mutant at right.

(B) and **(C)** Abaxial view of a cleared wild-type leaf **(B)** and a *Gn1-R* leaf **(C)** stained with toluidine blue. The arrows mark where intermediate veins anastomose with lateral veins at the ligule–auricle region. In **(C)**, vascular anastomosis takes place over a much longer region.

Two Arabidopsis mutants have been characterized that, like *Gn1-R*, are altered in leaf shape and have altered cell shapes. Leaves of the *angustifolia* mutant are narrower and thicker than wild-type leaves, and leaves of the *rotundifolia* mutant are wider and shorter. It is proposed that these genes function by regulating the polarity of cell shape (Tsuge et al., 1996). We have considered two possibilities for the relationship of cell shape and sheath morphology in *Gn1-R* mutants. Similar to the explanation for *angustifolia* and *rotundifolia*, *Gn1-R* may have a primary effect on cell shape that then influences leaf shape. Alternatively, *Gn1-R* may directly influence the overall morphology of the sheath, which then becomes partitioned into squatter, more irregularly shaped cells (Kaplan and Hagemann, 1991; Cooke and Lu, 1992; Smith et al., 1996). Clonal analysis of *Gn1-R* showed that sectors of wild-type tissue adjacent to mutant tissue were the same length as *Gn1-R* but were thinner in the transverse dimension (Foster et al., 1999). These results suggest that leaf thickness is specified at the cellular level; however, if leaf length is specified at the cellular level, then supracellular mechanisms can override that specification.

Ectopic Carpels Form in the Female Flower in *Gn1-R* Mutants

Gn1-R mutants have a floral defect in which extra carpels form around the central carpel. These carpelloid structures form late in development, after the stamen primordia have arrested in development and the silk of the central carpel has elongated. Although these structures often form in the position of stamen primordia, our double mutant analysis

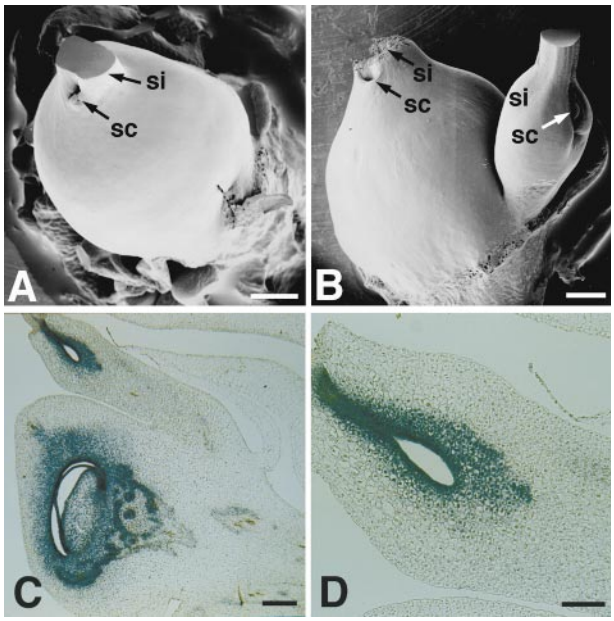

Figure 7. *Gn1-R* Female Flowers Have Extra Silk-Producing Structures.

(A) SEM of a wild-type female floret with glumes, lemma, and palea removed.

(B) SEM of a *Gn1-R* female floret. Extra silk-producing structures are growing out of the carpel wall.

(C) In situ localization in a *Gn1-R* female floret of *zag2*, a carpel-specific gene (Schmidt et al., 1993), indicates that the extra structure is carpelloid in identity.

(D) Higher magnification illustrates that the carpelloid organ has tissue organization similar to that of a normal pistil.

sc; stylar canal; si, silk. Bars in **(A)** and **(B)** = 600 μm; bars in **(C)** and **(D)** = 200 μm.

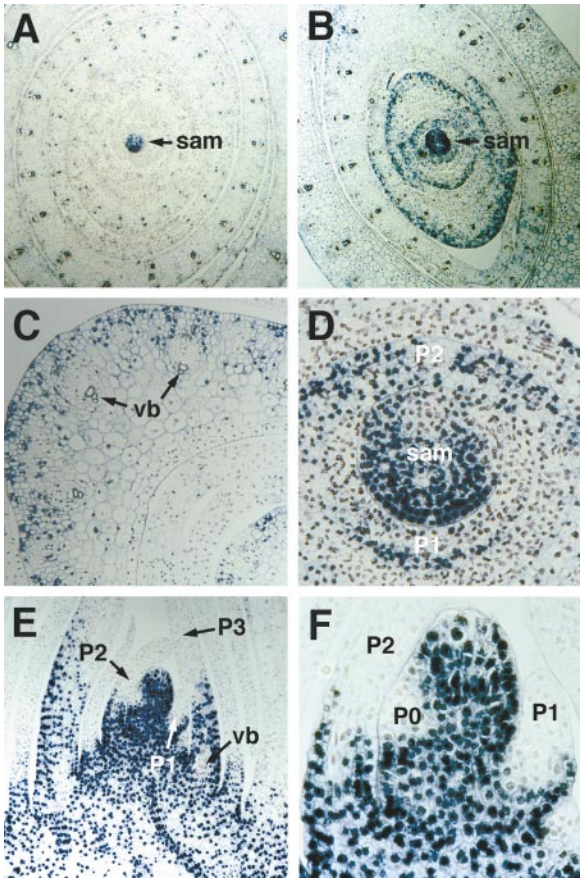

Figure 8. Immunohistochemical Analysis of Accumulation of KNOX Proteins in *Gn1-R* and Wild-Type Shoot Apices and Leaves.

(A) and **(B)** KNOX accumulation (dark blue nuclei) is seen in transverse sections through wild-type and *Gn1-R* shoot apical meristems, respectively. There was no detectable KNOX accumulation in wild-type leaves, but *Gn1-R* mutant leaves accumulated the KNOX protein along the abaxial side of leaves, near the midrib.

(C) Midrib of *Gn1-R* leaf at P_4, illustrating the accumulation of the KNOX protein.

(D) KNOX accumulation is apparent along the abaxial side of *Gn1-R* leaves as early as P_1.

(E) Median longitudinal section through a *Gn1-R* shoot apex, illustrating KNOX accumulation in the vegetative meristem and at the base of *Gn1-R* leaves during P_1 to P_6. No KNOX accumulation is detectable in more distal regions of *Gn1-R* leaves or in vascular elements.

(F) High-magnification image of *Gn1-R* shoot apical meristem pictured in **(E)**.

sam, shoot apical meristem; vb, vascular bundle.

does not support the idea that these extra carpels are transformed stamens.

A floral phenotype has not been noted for the dominant maize mutants; however, female flowers in the recessive *kn1* mutants have extra ovules, extra carpels, or protruding ovules (Kerstetter et al., 1997). These flowers are mainly sterile. The *Gn1-R*–conferred phenotype is distinct in that the central carpel is fertile and the extra carpels form ectopically from the outer wall. Ectopic organs and meristems have been described for dominant *kn1*-like mutants in barley and tomato and for barley, tobacco, and tomato plants that overexpress *kn1*. *Hooded* is a dominant mutation in barley that results from misexpression of a barley *kn1*-like gene, *HvKnox3* (Müller et al., 1995). Barley plants carrying the *Hooded* mutation and transgenic barley plants overexpressing *kn1* display ectopic inflorescence meristems along the awn, which is the extension of the lemma (Müller et al., 1995; Williams-Carrier et al., 1997). Tobacco plants overexpressing *kn1* occasionally display ectopic anther lobes on stamens, although the more consistent phenotype is ectopic meristems on vegetative leaves (Sinha et al., 1993). The dominant *Curl* mutant of tomato displays ectopic shoots on sepals in addition to other phenotypic anomalies (Parnis et al., 1997).

knox genes are strongly expressed in floral and inflorescence meristems, and they are downregulated as organs, including carpels, form (Smith et al., 1992; Jackson et al., 1994). A gene that may function to keep *knox* genes off in carpels is likely to be *rs2*. Recessive *rs2* mutants condition a phenotype similar to *Gn1-R* and *Rs1*, including the presence of ectopic carpels. Ectopic expression of *knox* genes has been demonstrated in *rs2* mutant leaves (Schneeberger et al., 1998). We predict that in *Gn1-R* mutants, the KNOX

```
KNOX4   1 MDQNFGNLGTGAGSSGGCGGSNSNSKAVAAVSSSSFLQLPLSTAAAASPA
          |||.|||||  |||||   |||||  .  |  ||||||||||||||   ||||
RS1     1 MDQSFGNLGAGAGSSS..GGSNSKA.AATAVSSSSFLQLPLST...ASPA

KNOX4  51 YYGAPLALLHHGTTAGPSSS..QQQQHQSPYAKHGAEMSAAEADAIKAKI
          ||||||||||||   |  ||   |||||   ||:||||||||||:||||||
RS1    45 YYGAPLALLHHAAAAPSSSQQHQQQQHHHHYARHGAEMSAAEAEAIKAKI

KNOX4  99 VAHPQYSALLAAYLDCQKVGAPPDLLERLTAMAAKLDARPPGRHGPRDPE
          |||||||||||||||||||||||.|||||||||||||   ||| |||||
RS1    95 VAHPQYSALLAAYLDCQKVGAPPDVLERLTAMAAKLDASAAGRHEPRDPE

KNOX4 149 LDQFMEAYCNMLVKYREELTRPIDEAMEFLKRVEAQLDSIAGGGSSSSAR
          |||||||||||||||||||||||||||||||||||||||| |.||| |||||
RS1   145 LDQFMEAYCNMLVKYREELTRPIDEAMEFLKRVEAQLDCISGGGGSSSAR

KNOX4 199 LSLADGKSSEGAGSSEDDDMDPSGRENEPPEIDPRAEDKELKYQLLKKYS
          ||||||| ||| |||| |||||.||||:||||||||||||||||||||||
RS1   195 LSLADGK.SEGVGSSE.DDMDPNGRENDPPEIDPRAEDKELKYQLLKKYS

KNOX4 249 GYLSSLRQEFSKKKKKGKLPKEARQKLLHWWELHYKWPYPSETEKIALAE
          ||||||||||||||||||||||||||||||||||||||||||||||||||
RS1   243 GYLSSLRQEFSKKKKKGKLPKEARQKLLHWWELHYKWPYPSETEKIALAE

KNOX4 299 ATGLDQKQINNWFINQRKRHWKPSEDMPFVMMEGFHPQTAAALYLDGGAF
          .|||||||||||||||||||||||||||||||||||||| |||||:| | |
RS1   293 STGLDQKQINNWFINQRKRHWKPSEDMPFVMMEGFHPQNAAALYMD.GPF

KNOX4 349 MADGMTTYRLGS
          | |||  |||||
RS1   342 MRDGM..YRLGS
```

Figure 9. Alignment of RS1 and KNOX4 Amino Acid Sequences.

A line between the amino acids indicates identical residues. There is a dot above every 10 amino acids. The homeodomain is underlined.

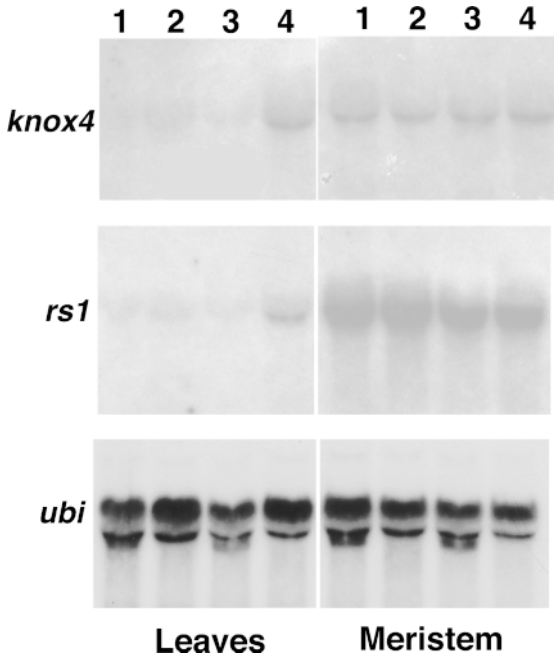

Figure 10. Expression of *knox4* in *Gn1-R* Leaves Is Decreased in Revertant Leaves (*Gn1-Rrev*).

Tissue was isolated from a segregating population of *Gn1-R* in a W22 background and a segregating population of *Gn1-Rrev* in a *Mutator* background. The *Gn1-R* and normal siblings were identified by phenotype. The *Gn1-Rrev* and normal siblings were identified using DNA gel blot analysis. Five to seven 2-week-old seedlings were dissected into leaf primordia and meristem-enriched tissue, as described previously (Mathern and Hake, 1997). Lanes 1, normal siblings from *Gn1-Rrev* family; lanes 2, normal siblings from *Gn1-R* family; lanes 3, *Gn1-Rrev* homozygous individuals; and lanes 4, *Gn1-R* individuals. The blot was probed with a *knox4* 3′ probe, a *rs1* 3′ probe (see Methods), and ubiquitin (*ubi*).

protein is ectopically expressed along the carpel wall after normal expression disappears, overriding the downregulation from regulators, such as RS2. Similar to the commitment of awn cells to a floral phenotype, we propose that the carpel cells ectopically expressing the KNOX protein are already committed to a carpel fate; therefore, they continue to proliferate carpel tissue.

Ectopic Expression of the KNOX Protein in *Gn1-R* Leaves

Immunolocalization experiments revealed the ectopic expression of KNOX protein in *Gn1-R* leaves as early as P_1. Ectopic expression is localized to the leaf base and is most intense near the midrib and toward the abaxial side of the leaf (Figure 8). The histological defects in *Gn1-R* sheath tissue are primarily focused on mesophyll cells in the abaxial layer. Thus, ectopic expression of KNOX protein in *Gn1-R* leaves is spatially and temporally correlated with the *Gn1-R* mutant phenotype.

This ectopic expression appears to manifest itself in two different ways: by altering the shape of sheath cells and by altering the cell identity in the region of the ligule. This finding suggests that only certain cells respond to the ectopic KNOX protein by cell fate changes. Cells of the blade can be transformed into sheath and ligule, as shown for *Kn1*, *Lg3*, and *Gn1* (Freeling and Hake, 1985; Sinha and Hake, 1994; Muehlbauer et al., 1997; Figure 5). Cells of the auricle region can become more sheathlike, as in *Rs1* mutants (Becraft and Freeling, 1994; Schneeberger et al., 1995), but sheath cells do not change their fate, only their shape. This restriction could be explained if the KNOX protein in leaves retards the normal course of differentiation but allows cells to adopt a leaf cell fate specified at a later stage. Because blade cells differentiate before sheath cells, blade cells that are unspecified have the opportunity to become sheath cells. Because

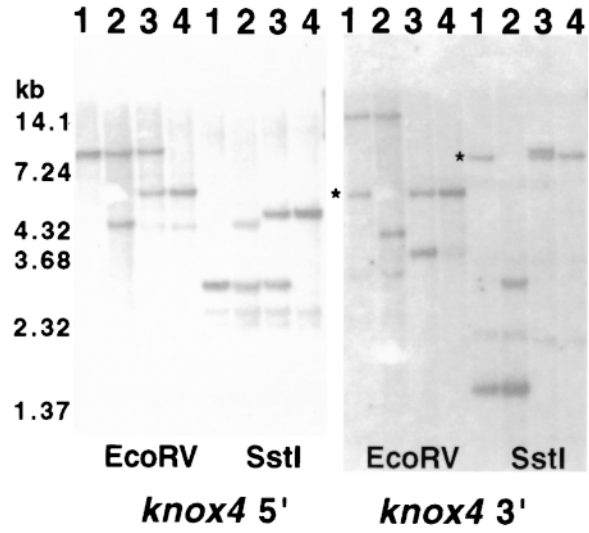

Figure 11. Genomic DNA Gel Blot Analysis of *Gn1-R* and the Revertant (*Gn1-Rrev*).

DNA was isolated from individuals with the following genotypes: (1) *Gn1-R*/*gn1*+, (2) *gn1*+/*gn1*+, (3) *Gn1-Rrev*/*gn1*+, and (4) *Gn1-Rrev*/*Gn1-Rrev*, as indicated above the gels. There are two different *gn1*+ alleles in these families. The blot was probed with a *knox4* 5′ probe (Bf3) and stripped and reprobed with a 3′ probe. The fragments specific to *Gn1-R* are altered in the *Gn1-Rrev* individuals when the blot is hybridized with a 5′ probe. The bands common to the *Gn1-R* individual and the revertants using the 3′ probe are indicated with asterisks. DNA length standards are given at left in kilobases.

sheath cells are the last to differentiate in the leaf, their fate cannot be respecified to another leaf cell type.

knox4 and *rs1* Are Likely to Be Duplicate Genes

The maize genome is thought to be derived from an ancient tetraploidization event, given that many genes hybridize to two map positions and that the gene order between these duplicated regions is often conserved (Wendel et al., 1986; Helentjaris et al., 1988; Gaut and Doebley, 1997). Three pairs of *knox* genes map to duplicated regions, including *knox4* and *rs1*, which map to chromosomes 2L and 7S, respectively (Kerstetter et al., 1994). The homeodomains of RS1 and KNOX4 are 100% identical, and the entire coding regions are 90% identical (Schneeberger et al., 1995; Figure 9). The mutant phenotypes of both *Gn1* and *Rs1* are similar, but each affects a distinct part of the leaf. Both *Gn1* and *Rs1* cause a transformation of the ligule region, but *Gn1* is unique because it also affects the entire length of the sheath. Ectopic *rs1* expression in *Rs1* leaves is localized to the base of leaves, around provascular elements (Schneeberger et al., 1995). Ectopic KNOX expression in *Gn1* leaves is also localized to the leaf base, but it does not appear to be expressed in provascular elements. Given the level of sequence identity, the slight difference in expression pattern could be important for the differences in phenotype.

Isolation of *knox* genes from rice has revealed that a single gene, *osh15*, is likely to correspond to *rs1* and *knox4* (Sato et al., 1999). The *osh15* nucleotide sequence is 70% identical to *rs1* and *knox4* throughout the coding region. In addition, *osh15* maps to a region of the rice genome at which synteny to chromosomes 2L and 7S of maize is observed (Ahn and Tanksley, 1993). Interestingly, the phenotype of an *osh15* deletion is similar to some aspects of the *Gn1-R*–conferred phenotype. The internodes of *osh15* mutants are short and squat, with a corresponding change in cell shape (Sato et al., 1999). Leaves in *osh15* mutants appear normal. These results could suggest that *Gn1-R* may be altered in its regulation such that it represses downstream targets that it normally activates. The repression of these targets would thus mimic the loss of an activator of the same targets.

The *Mu* element insertion into *knox4* reverted the *Gn1*-conferred phenotype but did not produce any other easily discernible phenotype (data not shown). Our results with *kn1* loss-of-function mutations have shown that the phenotype is very background dependent, implying the interaction of other genetic factors (Kerstetter et al., 1997; E. Vollbrecht, L. Reiser, and S. Hake, manuscript in preparation). It is also possible that the *Mu* insertion reverted the ectopic *knox4* expression without affecting the normal transcript. Future experiments will include screening for mobilization of the *Mu* insertion into *knox4* exons (Das and Martienssen, 1995) as well as determining the phenotype in different genetic backgrounds, including that of the *rs1* mutant.

METHODS

Maize Genetic Stocks

Gn1-R was a generous gift of T. Pryor. The mutant appeared as a single plant in a control population that was selected for the absence of *Activator* at the *PVV* locus. Anthers were dissected manually out of the male flowers of the mutant plant and outcrossed to a nonmutant female. *Liguleless–9167* was recovered by D. Schwartz and was made available by G. Muehlbauer and M. Freeling (University of California, Berkeley). Stocks carrying *silky* (*si*) and *silkless* (*sk*) mutations were provided by the Maize Genetics Stock Center (Urbana, IL). Heterozygous *Gn1-R* and *Gn1-S* plants were backcrossed to each inbred line for four to six generations. Mutant plants were used as male parents whenever possible. Individuals expressing a representative phenotype within a family (neither abnormally mild nor severe) were chosen for introgression. After four to six generations, the mutants expressed a very uniform phenotype within a given background.

Plant and Cell Measurements

Whole-plant height was measured from the lowest node (just above the tap root) to the tip of the tassel for 20 mutant and nonmutant siblings within a given background. Internode length was measured from node to node for each above-ground internode of 10 mutant and nonmutant siblings within a given background. Numbers were averaged and plotted as described above. Leaf dimension measurements were made of leaf 10 of 20 mutant and nonmutant siblings within a given background. Blade length was measured along the leaf margins, from the ligule to the tip. Sheath length was measured along leaf margins, from the point of insertion to the ligule. Blade and sheath widths were measured at the midpoint of each length. Numbers were averaged, and mutant dimensions were represented as a percentage of normal. A first-order Taylor expansion multivariate δ method was used to calculate the standard error for these measurements.

Epidermal replicas made using clear nail polish were then placed on glass microscope slides, covered with water and a glass cover slip, and viewed under a Zeiss Axiophot microscope (Thornwood, NY). Replicas were photographed at $\times$16 magnification, and the resulting 35-mm slides were scanned at 200% of the original image size. The scanned images were calibrated, and National Institutes of Health (Bethesda, MD) Image software was used to measure cell lengths of at least 80 cells per sample.

RNA and DNA Analyses

A genomic fragment, P11, corresponding to *knox4* (for *knotted1* [*kn1*]-like homeobox) was used to screen an ear cDNA library (Schmidt et al., 1993). CP11-5 was one of six clones that hybridized with P11. Genomic clones were isolated by screening a B73 MboI partial library (Clonetech, Palo Alto, CA), and four overlapping clones were identified. The full-length sequence of *knox4* was deduced by sequencing 5′ portions of the genomic clones. Sequence analysis and alignment were done using the Sequencher 3.0 and Genetics Computer Group (Madison, WI) programs.

RNA was isolated from 2-week-old seedlings, as described previously (Mathern and Hake, 1997). Total RNA samples were glyoxylated,

run on 1% agarose gels, and hybridized with the *knox4* cDNA (CP11-5). A gene-specific probe for *knox4* was prepared using the polymerase chain reaction (PCR) with the gn12 primer (5′-GTTCATCAACCAGCGG-3′) and the m13 −21 forward primer on CP11-5 plasmid DNA. The same primers were used on a *rough sheath1* (*rs1*) cDNA (CP11-6) to obtain an *rs1*-specific probe. These probes cross-hybridize to ~10% on test blots (J. Yamaguchi, unpublished data). The ubiquitin probe was a gift from P. Quail (Plant Gene Expression Center, Albany, CA) (Christensen et al., 1992).

DNA isolation and gel blot analysis have been described previously (Greene et al., 1994). The 5′ *knox4* probe is Bf3 (a 1.0-kb XbaI-SalI genomic fragment isolated from λ clone 5B1). PCR analysis on the revertants used gn117 (5′-agctcgagcgaacgcgatggtca-3′) and the *Mu* end primer Mu-9242 (5′-agagaagccaacgcca(a/t)cgcctc(c/t)atttcgtc-3′); the lowercase letters indicate a slight degeneracy.

Microscopy and in Situ Hybridization

Hand-cut sections were made, stained in a 1% acridine orange solution for 5 min, and then destained with several changes of water. Tissue was mounted in water on glass slides and observed with a Leica scanning laser confocal microscope at ×10 magnification. Samples were exposed to an excitation energy of 488 nm, and emitted light >510 nm was collected in one channel.

Leaf surfaces and pistillate flowers were examined by scanning electron microscopy (SEM) using the replica technique, as modified by Sylvester et al. (1990). Casts of epidermal surfaces were filled with high-strength epoxy. Epoxy replicas, polymerized for 24 to 48 hr, were mounted on SEM stubs and sputter coated with 25 nm of gold. The specimens were observed using a scanning electron microscope (model DS-130; ISI, Santa Clara, CA) operating at an accelerating voltage of 15 kV.

Gn1-R in a W22 background was grown to maturity in the field at Brentwood, CA. In situ hybridizations were performed with unfertilized ears that were harvested after silks had emerged from the husk leaves, as described by Jackson (1991). Probes were prepared from a 3′ subclone of the *zag2* (for *Zea mays AGAMOUS*) cDNA (Schmidt et al., 1993).

ACKNOWLEDGMENTS

We are indebted to Tony Pryor for providing us with the *Gn1-R* seed. We thank Drew Schwartz for giving the *Gn1-S* seed to Mike Freeling, and we thank Mike Freeling and Gary Muehlbauer for passing the seed on to us. We thank Leonore Reiser for ongoing help with figures and the manuscript and Allen Sessions and Paula McSteen for helpful criticisms. Thanks to members of both the Hake and Freeling laboratories for many stimulating discussions, especially Richard Schneeberger for sharing ideas as well as the KNOX antibody. Thanks to Denise Schichnes of the National Science Foundation Center for assistance with confocal imagery and Paula Sicurello for help at the Scanning Electron Facility at the University of California, Berkeley. The research was supported by U.S. Department of Agriculture National Research Initiative Grant No. 9701255 (to S.H.) and by the Marsden Foundation (to B.V.).

Received October 29, 1998; accepted April 6, 1999.

REFERENCES

Ahn, S., and Tanksley, S.D. (1993). Comparative linkage map of the rice and maize genomes. Proc. Natl. Acad. Sci. USA **90,** 7980–7984.

Becraft, P.W., and Freeling, M. (1994). Genetic analysis of *Rough sheath 1* developmental mutants of maize. Genetics **136,** 295–311.

Becraft, P.W., Bongard-Pierce, D.K., Sylvester, A.W., Poethig, R.S., and Freeling, M. (1990). The *liguleless-1* gene acts tissue specifically in maize leaf development. Dev. Biol. **141,** 220–232.

Brown, W.V. (1975). Variations in anatomy, associations and origins of Kranz tissue. Am. J. Bot. **62,** 395–402.

Chandler, V.L., and Hardeman, K. (1992). The *Mu* elements of *Zea mays*. Adv. Genet. **30,** 77–122.

Cheng, P.C., Greyson, R.I., and Walden, D.B. (1983). Organ initiation and the development of unisexual flowers in the tassel and ear of *Zea mays*. Am. J. Bot. **70,** 450–462.

Christensen, A.H., Sharrock, R.A., and Quail, P.H. (1992). Maize polyubiquitin genes: Structure, thermal perturbation of expression and transcript splicing, and promoter activity following transfer to protoplasts by electroporation. Plant Mol. Biol. **18,** 675–689.

Cooke, T.J., and Lu, B. (1992). The independence of cell shape and overall form in multicellular algae and land plants: Cells do not act as building blocks for constructing plant organs. Int. J. Plant Sci. **153** (suppl.), 7–27.

Das, L., and Martienssen, R. (1995). Site-selected transposon mutagenesis at the *hcf106* locus in maize. Plant Cell **7,** 287–294.

Foster, T., and Hake, S. (1994). It's a Gnarley one! (*Gn1*). Maize Genet. Coop. Newslett. **68,** 2.

Foster, T., Veit, B., and Hake, S. (1999). Mosaic analysis of the dominant mutant, *Gnarley1-R*, reveals distinct lateral and transverse signaling pathways during maize leaf development. Development **126,** 305–313.

Fowler, J.E., and Freeling, M. (1996). Genetic analysis of mutations that alter cell fates in maize leaves: Dominant *Liguleless* mutations. Dev. Genet. **18,** 198–222.

Fraser, A.C. (1933). Heritable characters of maize. XLIV. Silky ears. J. Hered. **24,** 41–46.

Freeling, M., and Hake, S. (1985). Developmental genetics of mutants that specify Knotted leaves in maize. Genetics **111,** 617–634.

Gaut, B.S., and Doebley, J.F. (1997). DNA sequence evidence for the segmental allotetraploid origin of maize. Proc. Natl. Acad. Sci. USA **94,** 6809–6814.

Greene, B., Walko, R., and Hake, S. (1994). *Mutator* insertions in an intron of the maize *knotted1* gene result in dominant suppressible mutations. Genetics **138,** 1275–1285.

Hake, S., Vollbrecht, E., and Freeling, M. (1989). Cloning *Knotted*, the dominant morphological mutant in maize using *Ds2* as a transposon tag. EMBO J. **8,** 15–22.

Harper, L., and Freeling, M. (1996). Interactions of *liguleless1* and *liguleless2* function during ligule induction in maize. Genetics **144,** 1871–1882.

Helentjaris, T., Weber, D., and Wright, S. (1988). Identification of the genomic locations of duplicate nucleotide sequences in maize by analysis of restriction fragment length polymorphisms. Genetics **118,** 353–363.

Irish, E.E., and Nelson, T.M. (1993). Development of *tassel seed 2* inflorescences in maize. Am. J. Bot. **80,** 292–299.

Jackson, D. (1991). In situ hybridization in plants. In Molecular Plant Pathology: A Practical Approach, D.J. Bowles, S.J. Gurr, and M. McPherson, eds (Oxford, UK: Oxford University Press), pp. 163–174.

Jackson, D., Veit, B., and Hake, S. (1994). Expression of maize *KNOTTED1*-related homeobox genes in the shoot apical meristem predicts patterns of morphogenesis in the vegetative shoot. Development **120,** 405–413.

Jones, D.F. (1925). Heritable characters of maize. XXIII. *Silkless*. J. Hered. **16,** 339–341.

Kaplan, D.R. (1973). The monocotyledons: Their evolution and comparative biology. VII. The problem of leaf morphology and evolution in the monocotyledons. Q. Rev. Biol. **48,** 437–457.

Kaplan, D.R., and Hagemann, W. (1991). The relationship of cell and organism in vascular plants. BioScience **41,** 693–703.

Kerstetter, R., Vollbrecht, E., Lowe, B., Veit, B., Yamaguchi, J., and Hake, S. (1994). Sequence analysis and expression patterns divide the maize *knotted1*-like homeobox genes into two classes. Plant Cell **6,** 1877–1887.

Kerstetter, R.A., Laudencia-Chingcuanco, D., Smith, L.G., and Hake, S. (1997). Loss of function mutations in the maize homeobox gene, *knotted1*, are defective in shoot meristem maintenance. Development **124,** 3045–3054.

Laughnan, J.R., and Gabay-Laughnan, S. (1993). The placement of genes using waxy-marked reciprocal translocations. In The Maize Handbook, M. Freeling and V. Walbot, eds (New York: Springer-Verlag), pp. 254–257.

Long, J.A., Moan, E.I., Medford, J.I., and Barton, M.K. (1996). A member of the KNOTTED class of homeodomain proteins encoded by the *SHOOT MERISTEMLESS* gene of *Arabidopsis*. Nature **379,** 66–69.

Marx, G.A. (1987). A suite of mutants that modify pattern formation in pea leaves. Plant Mol. Biol. Rep. **5,** 311–335.

Mathern, J., and Hake, S. (1997). *Mu* element–generated gene conversions in maize attenuate the dominant knotted phenotype. Genetics **147,** 305–314.

McHale, N.A. (1993). *Lam-1* and *Fat* genes control development of the leaf blade in *Nicotiana sylvestris*. Plant Cell **5,** 1029–1038.

Muehlbauer, G.J., Fowler, J.E., and Freeling, M. (1997). Sectors expressing the homeobox gene *liguleless3* implicate a time-dependent mechanism for cell fate acquisition along the proximal–distal axis of the maize leaf. Development **124,** 5097–5106.

Müller, K., Romano, N., Gerstner, O., Garcia-Maroto, F., Pozzi, C., Salamini, F., and Rohde, W. (1995). The barley *Hooded* mutation caused by a duplication in a homeobox gene intron. Nature **374,** 727–730.

Nelson, T., and Dengler, N. (1997). Leaf vascular pattern formation. Plant Cell **9,** 1121–1135.

Parnis, A., Cohen, O., Gutfinger, T., Hareven, D., Zamir, D., and Lifschitz, E. (1997). The dominant developmental mutants of tomato, *Mouse-Ear* and *Curl*, are associated with distinct modes of abnormal transcriptional regulation of a *Knotted* gene. Plant Cell **9,** 2143–2158.

Poethig, R.S. (1984). Cellular parameters of leaf morphogenesis in maize and tobacco. In Contemporary Problems in Plant Anatomy, R.A. White and W.C. Dickison, eds (New York: Academic Press), pp. 235–258.

Poethig, R.S. (1997). Leaf morphogenesis in flowering plants. Plant Cell **9,** 1077–1087.

Randolph, L.F. (1936). Developmental morphology of the caryopsis in maize. J. Agric. Res. **53,** 881–916.

Robertson, D.S. (1978). Characterization of a mutator system in maize. Mut. Res. **51,** 21–28.

Russell, S.H., and Evert, R.F. (1985). Leaf vasculature in *Zea mays* L. Planta **164,** 448–458.

Sato, Y., Sentoku, N., Miura, Y., Hirochika, H., Kitano, H., and Matsuoka, M. (1999). Loss of function mutations in the rice homeobox gene *OSH15* affect the architecture of internodes resulting in dwarf plants. EMBO J. **18,** 992–1002.

Scanlon, M.J., Schneeberger, R.G., and Freeling, M. (1996). The maize mutant *narrow sheath* fails to establish leaf margin identity in a meristematic domain. Development **122,** 1683–1691.

Schmidt, R.J., Veit, B., Mandel, M.A., Mena, M., Hake, S., and Yanofsky, M.F. (1993). Identification and molecular characterization of *ZAG1*, the maize homolog of the Arabidopsis floral homeotic gene *AGAMOUS*. Plant Cell **5,** 729–737.

Schneeberger, R.G., Becraft, P.W., Hake, S., and Freeling, M. (1995). Ectopic expression of the *knox* homeo box gene *rough sheath1* alters cell fate in the maize leaf. Genes Dev. **9,** 2292–2304.

Schneeberger, R.G., Tsiantis, M., Freeling, M., and Langdale, J.A. (1998). The *rough sheath2* gene negatively regulates homeobox gene expression during maize leaf development. Development **125,** 2857–2865.

Sharman, B.C. (1942). Developmental anatomy of the shoot of *Zea mays* L. Ann. Bot. **6,** 245–282.

Sinha, N., and Hake, S. (1994). The *Knotted* leaf blade is a mosaic of blade, sheath, and auricle identities. Dev. Genet. **15,** 401–414.

Sinha, N.R., Williams, R.E., and Hake, S. (1993). Overexpression of the maize homeo box gene, *KNOTTED-1*, causes a switch from determinate to indeterminate cell fate. Genes Dev. **7,** 787–795.

Smith, L.G., Greene, B., Veit, B., and Hake, S. (1992). A dominant mutation in the maize homeobox gene, *Knotted-1*, causes its ectopic expression in leaf cells with altered fates. Development **116,** 21–30.

Smith, L.G., Hake, S., and Sylvester, A.W. (1996). The *tangled-1* mutation alters cell division orientations throughout maize leaf development without altering leaf shape. Development **122,** 481–489.

Steeves, T.A., and Sussex, I.M. (1989). Patterns in Plant Development, 2nd ed. (Cambridge, UK: Cambridge University Press).

Sylvester, A.W., Cande, W.Z., and Freeling, M. (1990). Division and differentiation during normal and *liguleless-1* maize leaf development. Development **110,** 985–1000.

Sylvester, A.W., Smith, L., and Freeling, M. (1996). Acquisition of identity in the developing leaf. Ann. Rev. Cell Dev. Biol. **12,** 257–304.

Tsuge, T., Tsukaya, H., and Uchimiya, H. (1996). Two independent and polarized processes of cell elongation regulate leaf blade expansion in *Arabidopsis thaliana* (L.) Heynh. Development **122,** 1589–1600.

Veit, B., Schmidt, R.J., Hake, S., and Yanofsky, M.F. (1993). Maize floral development: New genes and old mutants. Plant Cell **5,** 1205–1215.

Vollbrecht, E., Veit, B., Sinha, N., and Hake, S. (1991). The developmental gene *Knotted-1* is a member of a maize homeobox gene family. Nature **350,** 241–243.

Wendel, J.F., Stuber, C.W., Edwards, M.D., and Goodman, M.M. (1986). Duplicated chromosome segments in maize (*Zea mays L.*): Further evidence from hexokinase isozymes. Theor. Appl. Genet. **72,** 178–185.

Williams-Carrier, R.E., Lie, Y.S., Hake, S., and Lemaux, P.G. (1997). Ectopic expression of the maize *kn1* gene phenocopies the *Hooded* mutant of barley. Development **124,** 3737–3745.